Defect solitons in two dimensional optical lattices with line defect

GUANG-YU JIANG[a,b*], YOU-WEN LIU[a]
[a]*Department of Applied Physics, Nanjing University of Aeronautics and Astronautics, Nanjing 210016, China*
[b]*Key Laboratory of Nondestructive Testing (Ministry of Education), Nanchang Hangkong University, Nanchang 330063, China*

The existence, stability and propagation properties of defect solitons in two-dimensional optical lattices with a line defect are investigated analytically and numerically. When line defects with various defect intensities are introduced into two-dimensional optical lattices, defect solitons can exist in different bandgaps. Some unique characteristics show that the line defect embedded into two-dimensional optical lattices can profoundly influence the shape, stability and propagation of solitons. For a positive defect, the solitons only exist in the semi-infinite gap and cannot be stable in the high power region. For a negative defect, the solitons can exist not only in the semi-infinite gap, but also in the first gap;the solitons are stable in the moderate power region in the first gap.

(Received February 14, 2012; accepted April 11, 2012)

Keywords: Nonlinear optics, Soliton propagation, Lattices

1. Introduction

Defect solitons are nonlinear defect modes that bifurcate out from the linear defect modes, such solitons exist in many branches of nonlinear science, including biology, photonic crystals, solid state physics, Bose-Einstein condensates, nonlinear optics and have many potential applications for the all-optical switch [1], the routing of optical signal [2], filtering [3], and steering of optical beams in lattices [4-6]. In experiments, defect solitons in both one-and two-dimensional (2D) photonic lattices have been successfully observed [7-17]. In particular, the positive and negative defects embedded in 2D optical lattices can also support various solitons such as fundamental, dipole, quadrupole, and vortex modes [18-23]. Recently, linear defect modes in 2D optical lattices with a negative defect have been reported experimentally [24]. Surface defect solitons have been experimentally observed in a hexagonal waveguide array in Kerr nonlinearity [25], and the existence and stability of defect solitons (DSs) in 2D square lattices with focusing nonlinearity have been reported [26]. Surface line defect gap soliton has only been mentioned, but an in-depth study on surface line defect gap soliton is comparatively lacked [27]. More recently, DSs in kagome optical lattices, DSs in triangular optical lattices, and surface line defect solitons (SLDSs) in 2D square optical lattices with defect line have been investigated theoretically [28-30]. In this paper, we reveal the existence of defect solitons in two-dimensional optical lattices with line defect and focusing saturable nonlinearity. The stability and propagation properties of solitons have been studied analytically and numerically. In uniform lattices, solitons exist in the semi-infinite gap, and they can be stable in the low power region. For a positive defect, the solitons still exist in the semi-infinite gap, and they cannot stably transmit in the high power region. For a negative defect, solitons can exist in the semi-infinite gap and in the first gap, solitons will be stable in the moderate power region in the first gap.

2. Model

Considering a light beam propagating along z axis and illuminating at the middle site of the line defect at the surface of two-dimensional optical lattices under focusing saturable nonlinearity, light transmission is governed by the following nonlinear Schrödinger equation [27,29]:

$$i\frac{\partial U}{\partial z}+\frac{\partial^2 U}{\partial x^2}+\frac{\partial^2 U}{\partial y^2}-\frac{E_0}{1+I_L+|U|^2}U=0 \qquad (1)$$

where U is the slowing varying amplitude of the probe beam and I_L is the intensity profile of two-dimensional optical lattices with a defect that described by

$$I_L=I_0\cos^2(x)\cos^2(y)\{1+\varepsilon\exp[-(x^2)^4/128]\} \qquad (2)$$

Here I_0 is the peak intensity of optical lattices. x (in unit of D/π) and z (in unit of $2k_lD^2/\pi^2$) is the transverse and longitudinal scale, respectively, in which $k_l=k_0n_e$, $k_0=2\pi/\lambda_0$ is the wave-number in vacuum (λ_0 is the wavelength in vacuum) and n_e is the unperturbed refractive index.E_0 (in

unit of $\pi^2/(k_0^2 n_e^4 D^2\gamma_{33})$) is the applied DC field voltage, where γ_{33} is the electrooptical coefficient of the crystal. ε is the modulation parameter of defect intensity, respectively. We take typical parameters in experimental conditions as shown in Refs. [24,27-29]: D=30 μm, d=5 μm, ε_1 =0.3, λ_0 =0.5μm, n_e=2.3, and γ_{33}=280 pm/V, then x =1,z =1,and E_0 =1 correspond to 9.55 μm, 5.5 mm, and 8.86 V/mm. Other parameters are I_0 =3, E_0 =6. Using the above parameters, we obtain the region of the semi-infinite gap as $\mu\leq$3.58, and the first gap as 4.41≤μ≤5.55 by the plane wave expansion method, the bandgap's structure shown in Fig. 1 (a). The intensity distributions of composite optical lattices with a positive defect (ε=0.5) and a negative defect (ε=-0.5) are displayed in Figs. 1(b) and 1(c), respectively.

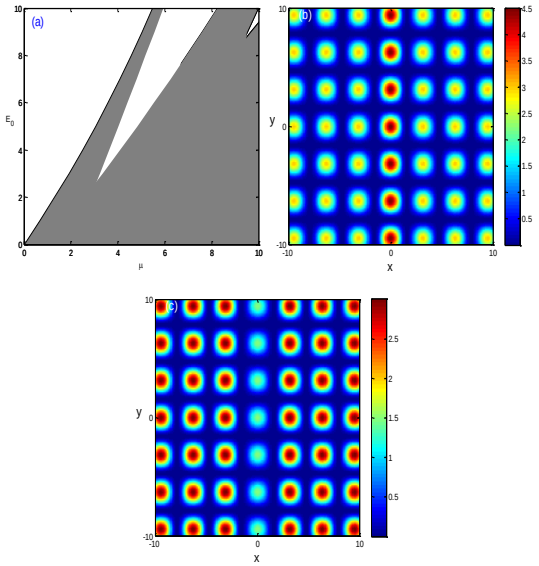

Fig. 1. (Color online.) (a) Band structure of square optical lattices. (b) the square optical lattices with a positive defect ε = 0.5, (c) the square optical lattices with a negative defect ε =-0.5.

To find the stationary solitons of Eq. (1), we first assume that $U=u(x,y)\exp(-i\mu z)$, where μ is the propagation constant, and $u(x,y)$ is the real function representing the profile of the soliton solution. Substituting the expression into Eq. (1) yields the following ordinary differential equation:

$$\frac{\partial^2 u}{\partial x^2}+\frac{\partial^2 u}{\partial y^2}-\frac{E_0}{1+I_L+|u|^2}u+\mu u=0 \quad (3)$$

The soliton solutions $u(x,y)$ can be solved numerically by a modified square-operator method [31, 32] and the power of solitons is defined as $P=\int_{-\infty}^{+\infty}\int_{-\infty}^{+\infty}|u|^2 dxdy$. To elucidate the stability of defect solitons in two dimensional optical lattices with line defect, we search for the perturbed solutions of Eq. (1) in the form

$$U(x,y,z)=\{u(x,y)+[v(x,y)-w(x,y)]\exp(\delta z)+[v(x,y)+w(x,y)]^*\exp(\delta^* z)\}\exp(-i\mu z) \quad (4)$$

where $v(x,y)$ and $w(x,y)$ are the real and imaginary part of infinitesimal perturbations, respectively, with a complex instability growth rate δ. The superscript "*" means complex conjugation, and $v(x,y),w(x,y)\ll 1$. Substituting Eq. (4) into Eq. (1) and linearizing, the eigenvalues of the coupled equations are obtained as

$$\begin{cases}\delta v=-i[\dfrac{\partial^2 w}{\partial x^2}+\dfrac{\partial^2 w}{\partial y^2}+\mu w-E_0 w/(1+I_L+u^2)] \\ \delta w=-i[\dfrac{\partial^2 v}{\partial x^2}+\dfrac{\partial^2 v}{\partial y^2}+\mu v-E_0 v(1+I_L-u^2)/(1+I_L+u^2)^2]\end{cases} \quad (5)$$

These equations can be solved numerically to obtain the perturbation growth rate Re (δ). If Re (δ)>0, solitons are linearly unstable. Otherwise, they are linearly stable.

3. Results and discussion

The robustness on propagation of the soliton is tested in direct simulations of Eq. (1) by adding a 10% rand noise perturbation to the inputted soliton. For a zero defect(ε=0), the power P of DSs versus propagation constant μ in Fig. 2(a).We can see that DSs only exist in the semi-infinite gap; their power gradually decreases with increasing of propagation constant μ and terminate at the semi-infinite band edges. In the region: μ<1.99, DSs cannot stably exist. As an example, the profiles of soliton for μ = 1.51 (point A in Fig. 2(a)) at different propagation distances (z=0, 50,100,150,200) are displayed in Fig. 2(c). In the moderate power region, we take μ = 1.8 (point B in Fig. 2(a)) for an unstable example. In such case, the soliton profiles of DSs at z=0, 50,100,150,200 are plotted in Fig. 2 (d). We can find in these figures that DSs can stably propagate for a small propagation distance; as the propagation distance z is further increased, DSs will obviously jump away from the initial site of soliton, and the shape of DSs is not centrosymmetric. To confirm the stability characteristics of DSs for the case of a zero defect (ε=0).In the low power region: 1.99≤ μ≤3.58, DSs can stably propagate. The solitons profile of a stable example (μ=2.35 corresponds to point C in Fig. 2(a)) is showed in Fig. 3(a). We can see that the shape of DSs can preserve its original shape; in the lower power region, we take (μ=3.25 corresponds to point D in Fig. 2(a)) for a stable example. In such case, the profiles of DSs at z=0, 50,100,150,200 are plotted in Fig.3 (b).We numerically calculate Eq. (5) to obtain the real part of perturbation growth rate Re (δ), as shown in Fig. 2(b). The Re(δ) is obviously larger than zero in the regions: μ<1.99,and DSs cannot stably transmit. However, in the region: μ<1.99, their slope of power diagram is negative, but Re(δ)>0.So we can conclude that this instability is different from the VK instability caused by the positive slope of power curve [33-36]. For the negative slope of power diagram (dP/dμ<0) and Re(δ) = 0 in the region:

1.99≤ μ≤3.58, the stability of DSs is in accordance with the VK criterion.

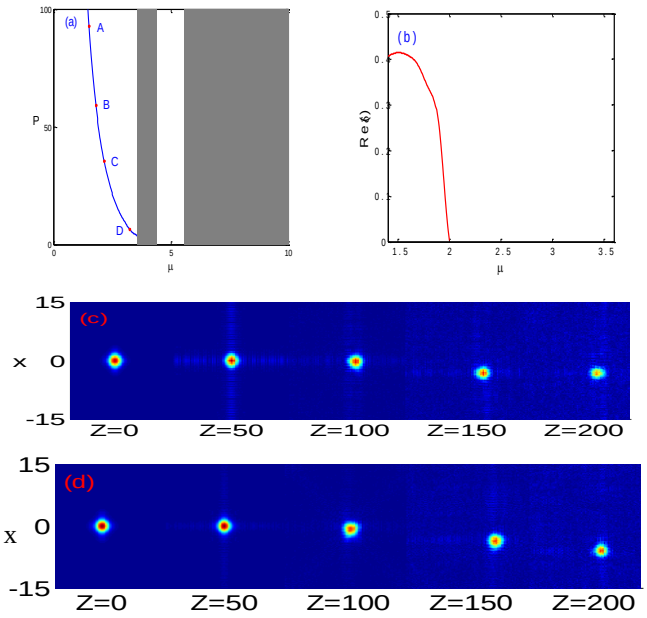

Fig. 2. (Color online.) ε = 0. (a) Power versus μ(gray regions corresponding to Bloch bands). (b) Re(δ) versus μ. (c) Profile (|u|) of DS for μ =1.51 (point A in (a)). Its profile (|u|) at z=0, 50,100,150,200. (d) Profile (|u|) of DS for μ =1.8(point B in (a)). Its profile (|u|) at z=0, 50, 100, 150, 200. The transverse domain is (-15,-15) × (-15,-15).

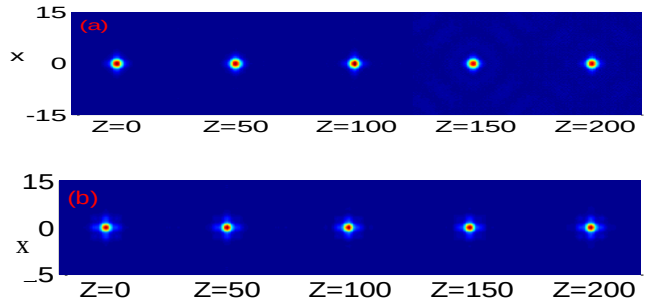

Fig. 3. (Color online.) ε=0. (a) Profile (|u|) of DS for μ=2.35 (point C). Its profile (|u|) at z=0, 50,100,150,200. (b) Profile (|u|) of DS for μ=3.25(point D). Its profile (|u|) at z = 0, 50, 100, 150, 200. The transverse domain is (-15,-15)×(-15,-15).

As a deeper defect considered, we choose a positive defect (ε=0.5). Fig. 4(a) presents the power *P* versus propagation constant μ for ε=0.5 at the surface of two-dimensional optical lattice with line defect. Note that their powers have the same trend with those for a zero defect (ε =0), but the power region will be narrower. As the increase of defect depth, DSs can still exist in the semi-infinite gap. The unstable regions of DSs in the semi-infinite gap are μ < 1.99 and 3.02<μ<3.31. As an unstable example, we select μ = 1.52 (point A in Fig. 4(a)) in the high power region: μ <1.99, DSs profiles at *z*=0, 50,100,150,200 are plotted in Fig. 4(c). The characteristics of instability in the Fig. 4(c) are the same with those in the Fig. 2 (d), but the shape of DSs cannot maintain and lose symmetry for propagation constant (μ = 1.52) in the unstable range. As another unstable example:μ=1.90 (point B in Fig. 4(a)) in the moderate power region, the unstable DSs propagations are shown in Fig. 4(d).DSs depart upward from the initial site at z=100,and downward for a longer propagation distance. As a stable example, the profile of DSs for μ =2.56 (point C in Fig. 4(a)) is shown in Fig. 5 (a). Fig. 5 (b) shows the unstable DSs profile for μ =3.15 (point D in Fig. 4(a)) in the low power. It makes clear that DSs can be trapped at the defect site for μ =2.56; as the propagation constant μ is increased to 3.15, DSs can be trapped at the defect site, but DSs cannot stably propagate for a longer distance. According to the relation of the Re(δ) and propagation constant μ, as shown in Fig. 4(b), we obtain the DSs'stable and unstable domains. In the region: 1.99≤ μ≤3.02, the slope of power curve and Re(δ) = 0,DSs can stably exist ,which accords with the VK criterion; while for Re (δ) > 0 and dP/dμ<0 at the region: 3.02<μ<3.31, DSs cannot stably exist, which is in agreement with "anti-VK" criterion. In addition, we also find that the light field concentrates together on the defect site mainly because a higher light intensity of positive defect attracts the light field, decreases the light diffraction and changes the stable region of DSs. With the effect of positive defect mode, DSs can stably propagate in the low power region of the semi-infinite gap.

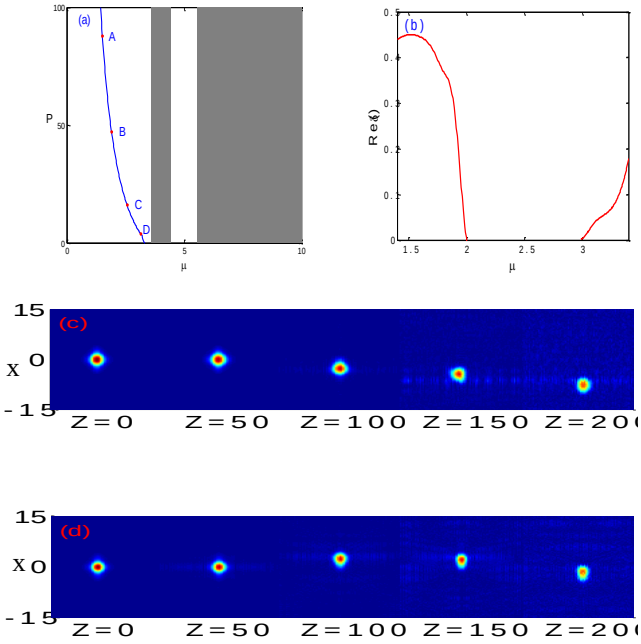

Fig. 4. (Color online.) ε = 0.5. (a) Power versus μ(gray regions corresponding to Bloch bands). (b) Re(δ) versus μ. (c) Profile (|u|) of DS for μ =1.52 (point A in (a)). Its profile (|u|) at z=0, 50,100,150,200. (d) Profile (|u|) of DS for μ = 1.90(point B in (a)). Its profile (|u|) at z=0, 50, 100, 150, 200. The transverse domain is (-15,-15) × (-15,-15).

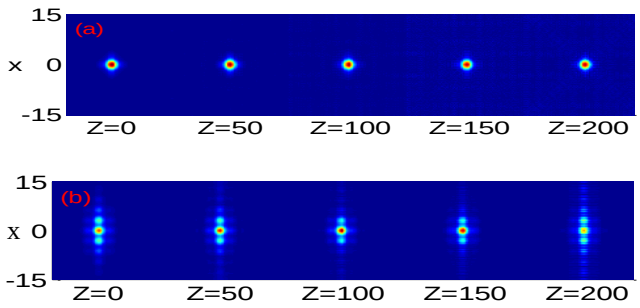

Fig. 5. (Color online.) ε=0.5. (a) Profile (|u|) of DS for μ=2.56 (point C). Its profile (|u|) at z=0, 50,100,150,200. (d) Profile (|u|) of DS for μ=3.15 (point D). Its profile (|u|) at z=0, 50,100,150,200. The transverse domain is (-15,-15)×(-15,-15).

As a typical case of the negative defect, we choose $\varepsilon=-0.5$, which is the same negative defect depth with these that in [26, 28-30]. In such case, the power P of DSs versus the propagation constant μ is shown in Fig. 6(a). From this figure, DSs cannot only exist in the semi-infinite gap but also in the first gap; the power of DSs decreases with the increase of propagation constant μ,but abruptly change nearby the semi-infinite gap. Unlike the characteristics in[26],where DSs can not only exist in the semi-infinite gap but also in the first gap, and the DSs show different stable and unstable regions in different gaps. In [28], in the semi-infinite gap, the stable regions are $2.42\leq\mu\leq3.33$, respectively, where the power of DSs is moderate. In [29], the solitons can be stable in the region: $4.16\leq\mu\leq6.05$ in the semi-infinite gap. In [30], the surface line defect solitons in the square lattices can be stable in the region: $2.18\leq\mu\leq3.13$ in the semi-infinite gap. However, the DSs in triangular lattices are not stable in the semi-infinite gap. Comparing with those, the DSs in two-dimensional optical lattice with line defect can exist in the semi-infinite gap and in the first gap. The stable regions are $2.49\leq\mu\leq3.30$ in the semi-infinite gap, but DSs are not stable in the regions: $\mu>2.49$ and $3.30<\mu<3.58$, respectively. We choose $\mu=1.53$(point A in Fig. 6(a)) as an example of unstable soliton in the high power range, whose profiles at z=0, 50,100,150,200 are shown in Fig. 6(c). In the high power, DSs cannot propagate stably. With the increase of propagation distance, DSs drift away from the initial place. The shape of DSs will change after this process. As another typical unstable example: $\mu=1.89$ (point B in Fig. 6(a)) in the moderate power. The profiles of DSs at the above propagation distances are presented in Fig. 6(d), where DSs cannot maintain its profile during propagation. When $2.49\leq\mu\leq3.30$, the power of DSs is linear change with the increasing of propagation constant μ. that means DSs in the region can stably propagate. As an example, we give the profile of DSs for $\mu=3.17$ (point C in Fig. 6(a)) in the low power. DSs at z=0, 50,100,150,200 can be trapped at the defect site in Fig. 6 (e). Fig. 6 (b) shows the change of the Re(δ) with propagation constant μ. For Re(δ)>0 in the region: $\mu>2.49$ and $3.30<\mu<3.58$,the DSs cannot stably propagate. In the moderate power region: $2.49\leq\mu\leq3.30$,the slope of power curve is negative and Re(δ)=0, the stability of DSs in this region satisfies the VK criterion. In the first gap, the solitons profile of a stable example ($\mu=4.55$ corresponds to point D in Fig. 6(a)) is showed in Fig. 6(f). We will show the stable DSs propagation in this region. We also can find in these figures that the shape of stable DSs in the first gap is very different from that in the semi-infinite gap. For dP/dμ <0 in the first gap that is obtained form the gradually decreasing power of DSs with the increasing of the propagation constant μ, we can conclude that the stability of DSs in the firs gap is in accordance with the VK criterion.

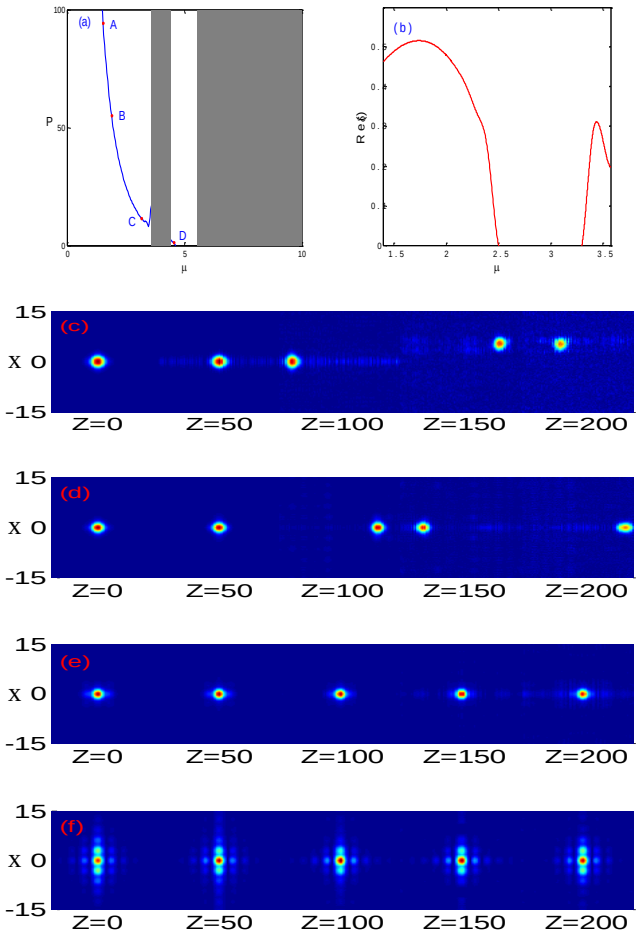

Fig. 6. (Color online.) ε=-0.5. (a) Power versus μ(gray regions corresponding to Bloch bands). (b) Re(δ) versus μ.(c) Profile (|u|) of DS for μ =1.53 (point A in (a)). Its profile (|u|) at z=0, 50,100,150,200. (d) Profile (|u|) of DS for μ = 1.89(point B in (a)). Its profile (|u|) at z=0, 50,100,150,200. (e) Profile (|u|) of DS for μ =3.17 (point C in (a)). Its profile (|u|) at z=0, 50,100,150,200.(f) Profile (|u|) of DS for μ =4.55 (point D in (a)). Its profile (|u|) at z=0, 50,100,150,200. The transverse domain is (-15,-15)×(-15,-15).

4. Conclusions

In summary, the existence, stability and propagation dynamics of DSs in two-dimensional optical lattices with line defect with focusing saturable nonlinearity have been revealed and investigated numerically. The results show that, as the line defects introduced in optical lattices, DSs can exist in different gaps, propagate stably and unstably in different power regions, and show abundant properties upon propagation. For a zero defect, the gap solitons exist only in the semi-infinite gap, and can be stable in the low power region. For a positive defect, DSs can exist only in the semi-infinite gap, and cannot stably transmit in the high power region. For a negative defect, DSs cannot only exist in the semi-infinite gap but also in the first gap, and can stably propagate in the moderate power region in the first gap.

Acknowledgments

This work was supported by the Scientific Research Foundation for the Returned Overseas Chinese Scholars, Specialized Research Fund for the Doctoral Program of Higher Education (200802871028), and the Summit of the "Six Great Talents" of Jiangsu Province (07-A-011).

References

[1] F. Ye, Y. V. Kartashov, V. A. Vysloukh, L. Torner, Phys. Rev. A **78**, 013847 (2008).
[2] Y. V. Kartashov, V. A. Vysloukh, L. Torner, Progress in Optics **52**, 63 (2009).
[3] A. A. Sukhorukov, Y. S. Kivshar, Opt. Lett. **30**, 1849 (2005).
[4] C. R. Rosberg, I. L. Garanovich, A. A. Sukhorukov, D. N. Neshev, W. Krolikowski, Y. S. Kivshar, Opt. Lett. **31**, 1498 (2006).
[5] A. Piccardi, G. Assanto, L. Lucchetti, F. Simoni, Appl. Phys. Lett. **93**, 171104 (2008).
[6] Y. V. Kartashov, L. Torner,Victor A. Vysloukh, Opt. Lett. **29**, 1102 (2004).
[7] L. X. Zheng, X. Zhu, H. G. Li, Y. J. He, J. Opt. Soc. Am. B.**28**, 2070 (2011).
[8] J. N. Xie, Y. J. He, H. Z. Wang, J. Opt. Soc. Am. B. **27**, 484 (2010).
[9] Y. J. He, D. Mihalache, B. Hu, Opt. Lett. **35**, 1716 (2010).
[10] W. L. Zhu, L. Luo, Y. J. He, H. Z. Wang, Chinese Physics B **18**, 4319 (2009).
[11] W. L. Zhu, L. Luo, Y. J. He, J. Modern Optics **56**, 1078 (2009).
[12] W. H. Chen, Y. J. He, H. Z. Wang, Phys. Lett. A **372**, 3525 (2008).
[13] S. Suntsov, K. G. Makris, G. A. Siviloglou, R. Iwanow, R. Schiek, D. N. Christodoulides, G. I. Stegeman, R. Morandotti, H. Yang, G. Salamo, M. Volatier, V. Aimez, R. Arès, M. Sorel, Y. Min, W. Sohler, X. Wang, A. Bezryadina, Z. Chen, J. Nonlinear Opt. Phys. Mater. **16**, 401 (2007).
[14] F. Fedele, J. Yang, Z. Chen, Opt. Lett. **30**, 1506 (2005).
[15] M. J. Ma, R. Carretero, P. G. Kevrekidis, D. J. Frantzeskakis, B. A. Malomed, Phys. Rev. A.**82**, 023621 (2010).
[16] M. Heinrich, Y. V. Kartashov, L. P. R. Ramirez, A. Szameit, F. Dreisow, R. Keil, S. Nolte, A. Tünnermann, V. A. Vysloukh, L. Torner, Opt. Lett. **34**, 3701(2009).
[17] J. Yang, I. Makasyuk, A. Bezryadina, Z. Chen, Stud. Appl. Math. **113**, 389 (2004).
[18] J. Yang, Ziad H. Musslimani, Opt. Lett. **28**, 2094 (2003).
[19] Y. V. Kartashov, B. A. Malomed, V. A. Vysloukh, L. Torner, Opt. Lett. **34**, 770(2009).
[20] B. B. Baizakov, B. A. Malomed, M. Salerno, Europhys. Lett. **63**, 642 (2003).
[21] J. Wang, Y. Yang, Phys. Rev. A **77**, 033834 (2008).
[22] J. Yang, I. Makasyuk, A. Bezryadina, Z. Chen, Stud. Appl. Math. **113**, 389 (2004).
[23] Y. V. Kartashov, A. Ferrando, A. A. Egorov, L. Torner, Phys. Rev. Lett. **95**, 123902 (2005).
[24] I. Makasyuk, Z. Chen, J. Yang, Phys. Rev. Lett. **96**, 223903 (2006).
[25] A. Szameit, Y. V. Kartashov, M. Heinirich, F. Dreisow, T. Pertsch, S. Nolte, A. Tünnermann, F. Lederer, V. A. Vysloukh, L. Torner, Opt. Lett. **34**, 797 (2009).
[26] W. H. Chen, X. Zhu, T. W. Wu, R. H. Li, Opt. Express **18**, 10956 (2010).
[27] Y. Li, W. Pang, Y. Chen, Z. Yu, J. Zhou, H. Zhang, Phys. Rev. A**80**, 043824 (2009).
[28] X. Zhu, H. Wang, L. X. Zheng, Opt. Express **18**, 20786 (2010).
[29] X. Zhu, H. Wang, T. W. Wu, L. X. Zheng, J. Opt. Soc. Am. B **28**, 521 (2011).
[30] Z. E. Lu, Z. M. Zhang, Opt. Express **19**, 2410 (2011).
[31] J. Yang, T. I. Lakoba, Stud. Appl. Math. **118**, 153 (2007).
[32] J. Yang, J. Comput. Phys. **277**, 6862 (2008).
[33] J. W. Fleischer, M. Segev, N. K. Efremidis, D. N. Christodoulides, Nature **422**,147 (2003).
[34] H. Sakaguchi, B. A. Malomed, Phys. Rev. A **81**, 013624 (2010).
[35] J. Yang, Z. Chen, Phys. Rev. E **73**, 026609 (2006).
[36] I. M. Merhasin, B. V. Gisin, R. Driben, B. A. Malomed, Phys. Rev. E **71**, 016613 (2005).

*Corresponding author: jgy579@126.com